Development 138, 3387-3397 (2011) doi:10.1242/dev.066340

CaMK-II is a PKD2 target that promotes pronephric kidney development and stabilizes cilia

Sarah C. Rothschild, Ludmila Francescatto, Iain A. Drummond[1] and Robert M. Tombes[2,*]

SUMMARY

Intracellular Ca^{2+} signals influence gastrulation, neurogenesis and organogenesis through pathways that are still being defined. One potential Ca^{2+} mediator of many of these morphogenic processes is CaMK-II, a conserved calmodulin-dependent protein kinase. Prolonged Ca^{2+} stimulation converts CaMK-II into an activated state that, in the zebrafish, is detected in the forebrain, ear and kidney. Autosomal dominant polycystic kidney disease has been linked to mutations in the Ca^{2+}-conducting TRP family member PKD2, the suppression of which in vertebrate model organisms results in kidney cysts. Both PKD2-deficient and CaMK-II-deficient zebrafish embryos fail to form pronephric ducts properly, and exhibit anterior cysts and destabilized cloacal cilia. PKD2 suppression inactivates CaMK-II in pronephric cells and cilia, whereas constitutively active CaMK-II restores pronephric duct formation in *pkd2* morphants. PKD2 and CaMK-II deficiencies are synergistic, supporting their existence in the same genetic pathway. We conclude that CaMK-II is a crucial effector of PKD2 Ca^{2+} that both promotes morphogenesis of the pronephric kidney and stabilizes primary cloacal cilia.

KEY WORDS: CaMK-II, PKD2, Cilia, Kidney, ADPKD, Zebrafish

INTRODUCTION

Although roles for Ca^{2+} signaling during early development have been supported by a rich and influential history of inquiry (Whitaker, 2006), the identification of the responsible Ca^{2+}-dependent molecular targets has remained elusive. For example, cellular behaviors during gastrulation, somitogenesis and trunk, eye, brain and organ formation have been associated with Ca^{2+} flux through specific channels (Porter et al., 2003; Webb and Miller, 2003; Webb and Miller, 2007; Whitaker, 2006), but have not been attributed to specific Ca^{2+}-dependent effectors.

CaMK-II, the Ca^{2+}/calmodulin-dependent protein kinase type II, is best known as an enzyme enriched in the central nervous system and important for long-term potentiation (Hudmon and Schulman, 2002). CaMK-II has also been implicated in embryonic cell migration (Easley et al., 2008), cell cycle progression (Rasmussen and Rasmussen, 1995; Tombes et al., 1995) and convergent cell movement in response to non-canonical Wnt signals (Kühl et al., 2000). CaMK-II has recently been identified as an essential Ca^{2+} target in the zebrafish Kupffer's vesicle (KV), the ciliated organ necessary for establishment of left-right asymmetry (Francescatto et al., 2010). Cilia in developing tissues have emerged as signaling centers, whose functions hold important clues to human ciliopathies (Fliegauf et al., 2007; Lancaster and Gleeson, 2009; Veland et al., 2009).

Polycystic kidney disease is a ciliopathy that can be linked to defects in Ca^{2+} signaling. Autosomal dominant polycystic kidney disease (ADPKD) is the most common monogenetic kidney disease affecting one in 1000 births, typified by the development of massive kidney cysts and caused by mutations in the polycystins, PKD1 or PKD2 (Wilson, 2004). PKD1 is a large receptor-like integral membrane protein with an extracellular N-terminus that contains motifs for cell-cell and cell-matrix interactions (Torres et al., 2007). PKD2 is a member of the TRP superfamily of nonselective Ca^{2+}-permeable ion channels (Clapham, 2003) found in the plasma membrane, the endoplasmic reticulum and in the primary cilium (Cai et al., 1999; Tsiokas, 2009). Both PKD1 and PKD2 contain coiled-coil domains in their intracellular C-terminus that enables the formation of a receptor-channel complex (Casuscelli et al., 2009; Giamarchi et al., 2010; Qian et al., 1997; Tsiokas et al., 1997). This complex is thought to play a role in regulating levels of intracellular Ca^{2+}, where activation of PKD1 induces Ca^{2+} entry via PKD2 (Hanaoka et al., 2000; Vandorpe et al., 2001). Mice homozygous for mutations in *Pkd2* develop cardiac abnormalities, situs inversus and cysts in the kidney and pancreas and die before E16.5 (Pennekamp et al., 2002; Wu et al., 2000). Suppression of *pkd2* in zebrafish results in hydrocephaly, loss of left-right asymmetry, body curvature, pronephric occlusions and pronephric cysts (Bisgrove et al., 2005; Obara et al., 2006; Schottenfeld et al., 2007; Sun et al., 2004). Dominant-negative PKD2 causes zebrafish and rat kidney cysts (Feng et al., 2008; Gallagher et al., 2006). Interestingly, Ca^{2+}-channel blockade increases cystic development in a PKD rat model, whereas a Ca^{2+} mimetic inhibits late stage cystogenesis (Gattone et al., 2009; Nagao et al., 2008). In summary, diminished activation of both intracellular Ca^{2+} signals and presumptive downstream Ca^{2+} targets leads to kidney cyst formation.

In this study, activated CaMK-II was detected during early zebrafish development in specific ciliated tissues including cells of the nervous system, the inner ear and pronephric kidney. In the developing kidney, CaMK-II activation was found to be dependent on PKD2 Ca^{2+} and was capable of restoring proper kidney development in PKD2-deficient embryos. These findings indicate that CaMK-II is a natural transducer of PKD2 Ca^{2+} to enable both anterior ductal cell migration and cloacal cilia stability. These findings have implications to other ciliated tissues and identify a potential new therapeutic target for ADPKD.

[1]Nephrology Division, Massachusetts General Hospital, Charlestown, MA 02129, USA. [2]Department of Biology, Virginia Commonwealth University, Richmond, VA 23284-2012, USA.

*Author for correspondence (rtombes@vcu.edu)

Accepted 31 May 2011

MATERIALS AND METHODS

Zebrafish strains and care

Wild-type (AB and WIK), Tg(α1 subunit Na^+/K^+-ATPase-GFP) and Tg(β-actin:CAAX-GFP) zebrafish (*Danio rerio*) embryos were obtained through natural matings and raised at 28.5°C as previously described (Kimmel et al., 1995).

In situ hybridization

Digoxigenin-labeled antisense riboprobes (0.5-1.5 kb) were synthesized using T3 or T7 RNA polymerase from cloned cDNAs and then hybridized with fixed embryos as previously described (Rothschild et al., 2007). For whole-mount in situ hybridization, embryos were developed using alkaline phosphatase-conjugated anti-digoxigenin. *gata3*, *cdh17*, *wt1a*, *pax2a* and *ret1* probes were prepared as previously described (Wingert and Davidson, 2008; Wingert et al., 2007). A γ1c antisense probe was generated from 48 hours postfertilization (hpf) kidney cDNA, TOPO cloned, linearized with *Not*I and transcribed using the T3 RNA polymerase. Fluorescent in situ hybridization was conducted as previously described (Rothschild et al., 2007) using fluorescent anti-digoxigenin antibodies and images were acquired using a Nikon C1 laser scanning confocal microscope.

CaMK-II antibodies

Immunolocalization using anti-phosphorylated CaMK-II (anti-P-CaMK-II; phosphorylated at Thr^{287}), CaMK-II and total CaMK-II antibodies has previously been described by this laboratory (Easley et al., 2006; Francescatto et al., 2010). The anti-phospho-Thr^{287} (anti-P-T^{287}) antibody detects CaMK-II proteins across species and the total CaMK-II antibody reacts with the C-terminal region of all CaMK-II proteins.

Pronephric dissection and flow sorting

Na^+/K^+-ATPase-GFP transgenic embryos at 24, 48 and 72 hpf were anesthetized and the pronephros dissected as previously described (Liu et al., 2007). Dissected pronephroi were dissolved in TRIzol reagent (Invitrogen) to prepare RNA, or harvested for CaMK-II activity assays as previously described (Rothschild et al., 2009; Rothschild et al., 2007). For flow sorted kidney cells, embryos were incubated in collagenase (Kramer-Zucker et al., 2005), then placed into 0.25% trypsin-EDTA for 30 minutes at 28.5°C. Embryos were filtered through mesh before sorting on a Becton-Dickinson FACS Aria II high-speed analyzer/sorter. RNA was prepared from Na^+/K^+-ATPase-GFP-positive cells.

CaMK-II activity assay

Whole embryos were lysed or GFP-expressing pronephroi were obtained and total CaMK-II activity was assessed by measuring phosphate incorporation into the substrate autocamtide-2, as previously described (Rothschild et al., 2007).

Immunolocalization

Embryos were fixed in 4% paraformaldehyde in PBS alone for F-actin staining, or in conjunction with methanol for P-CaMK-II, total CaMK-II and acetylated tubulin immunostaining. Dent's fixative (80:20 methanol:DMSO) was used for immunostaining the α1 subunit of Na^+/K^+-ATPase (α6F), atypical protein kinase C (aPKC) and γ-tubulin. Embryos were incubated with rabbit anti-P-T^{287} (Millipore; 1:20), mouse anti-total CaMK-II (BD Biosciences; 1:20), mouse anti-acetylated α-tubulin antibody (Sigma Chemical Co.; 1:500), mouse anti-α6F (Developmental Studies Hybridoma Bank, University of Iowa; 1:10), rabbit anti-aPKC (Santa Cruz; 1:10), or rabbit or mouse anti-γ-tubulin (Sigma Chemical Co.; 1:500) followed by either goat anti-mouse Alexa Fluor 488, goat anti-mouse Alexa Fluor 568, or goat anti-rabbit Alexa Fluor 568 (Invitrogen; 1:500). Embryos were permeabilized with NP-40 before staining F-actin with Alexa-Fluor-488-phalloidin (Invitrogen; 1:500). Embryos were imaged using confocal microscopy (Nikon C1 Plus two-laser) on a Nikon E-600 compound microscope using a 20× or 40× dry or 100× oil immersion objective.

Morpholino oligonucleotide and cDNA injections

The zebrafish *pkd2* morpholino oligonucleotide (MO; 4 ng), the *camk2g1* MO (1 ng) and the control mismatch MO (1 ng) were purchased from GeneTools and used as previously described (Francescatto et al., 2010), with a constant injection volume of 1 nl. Wild-type (WT) or T^{287}D CaMK-II δ_E were co-injected with the MO as previously described (Rothschild et al., 2009). Kidney-targeted WT and K^{43}A CaMK-II δ_E CaMK-II using the Na^+/K^+-ATPase promoter (Liu et al., 2007) were generated using Gateway technology (Invitrogen) (Francescatto et al., 2010).

Renal filtration

Renal filtration assays used tetramethylrhodamine dextran (70,000 MW; Invitrogen) injected into the pericardial sac of transiently anesthetized [0.003% Tricaine (MS-222); Sigma] 56 hpf zebrafish embryos as previously described (Tobin and Beales, 2008). Embryos were imaged within 20 minutes of injection and then again at 72 hpf. Six of the seven control embryos, but none of the eight *camk2g1* morphants, showed >50% reduction in rhodamine-dextran from the pericardial sac and anterior embryo.

Vibratome sections

Zebrafish embryos at 3dpf were fixed in 4% paraformaldehyde for 4 hours at room temperature and washed several times in PBT. The yolks were punctured and embryos were embedded in 5% low melting point agarose (Sigma). 100 μm sections were obtained using a Leica VT1000P vibratome and then labeled with 10 μg/ml propidium iodide (Sigma) and Alexa-Fluor-488-phalloidin (1:500). Sections were mounted in 50% glycerol in PBT between coverslips and imaged using confocal microscopy.

High-speed video microscopy

Live embryos were imaged using differential interference contrast optics after transient anesthesia and immobilization in low melting point agarose. Ciliary motility was imaged in the pronephric duct and cloaca in anesthetized embryos using a Nikon 60× water immersion Plan APO objective with DIC optics and 20 frames per second acquisitions. Lengths of cilia in fixed embryos were determined from anti-acetylated α-tubulin whole mounts using quantitative length algorithms in Nikon Elements software. For each condition, two to five experimental replicates were examined with total embryo numbers between 20 and 40. Statistical analyses were performed using the paired *t*-test. Statistical significance was set at $P<0.005$.

RESULTS

CaMK-II is most often linked to central nervous system function, where it can constitute as much as 1% of the total protein (Hudmon and Schulman, 2002). However, CaMK-II is expressed in every adult mammalian tissue (Tobimatsu and Fujisawa, 1989) and across all metazoan species (Tombes et al., 2003). CaMK-II is different from other CaM-dependent kinases because it is able to oligomerize and autophosphorylate at T^{287} upon prolonged Ca^{2+}/CaM stimulation. T^{287} autophosphorylation converts CaMK-II into a Ca^{2+}-independent state. Activated (P-T^{287}) CaMK-II has been detected in zebrafish embryos as early as the 10-somite stage (Francescatto et al., 2010), but it is also found in the forebrain, in a region corresponding to the olfactory placode, in the pronephric duct and cloaca, and at the base of inner ear hair cell kinocilia (Fig. 1). These locations are a subset of total CaMK-II expression in the embryonic forebrain, olfactory placode, spinal cord, somites, pectoral fins, ear and pronephric kidney, as determined immunologically (Fig. 1) and by in situ hybridization (Rothschild et al., 2009; Rothschild et al., 2007). At 60 hpf, CaMK-II remains activated in kidney and ear cells and becomes activated in retina, anterior pituitary and neuromasts of the lateral line (Fig. 2).

Differential activation of CaMK-II along the zebrafish kidney

The preferential activation of CaMK-II in the developing kidney was confirmed in dissected 3 dpf pronephric kidneys compared with 6 dpf whole embryos (Fig. 3A). In whole mounts, CaMK-II activation varied along the pronephros (Fig. 3B). The pronephric

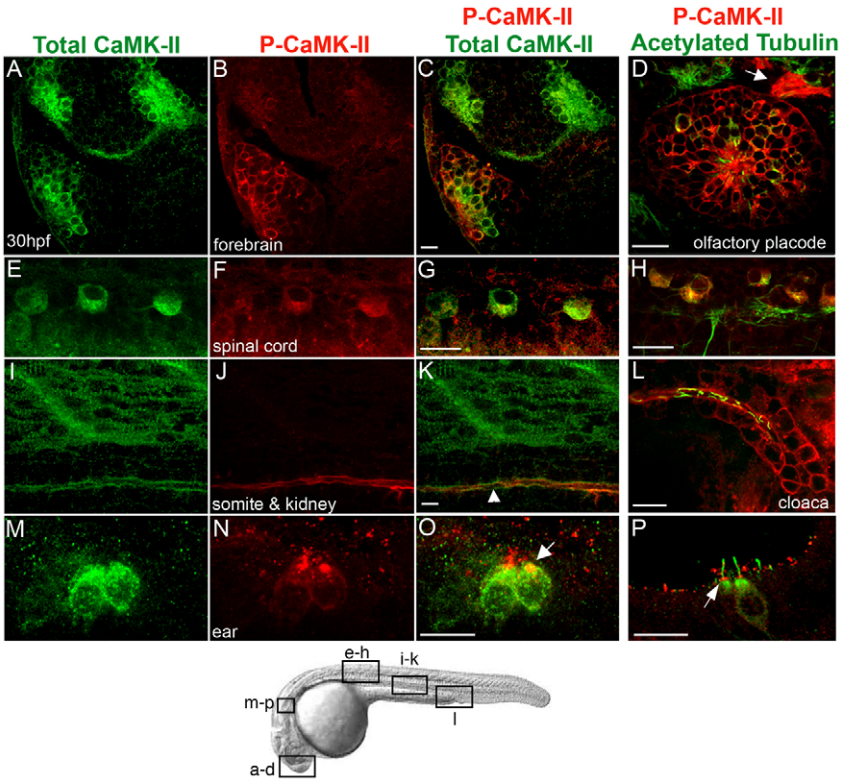

Fig. 1. Localization of activated and total CaMK-II in 30 hpf zebrafish embryos. (**A-P**) Embryos were immunolabeled for total CaMK-II (A,E,I,M) and P-CaMK-II (B,F,J,N) and imaged laterally in the forebrain (A-C), spinal cord cell bodies (E-G), muscle sarcomeres and the pronephric kidney (I-K), and embryonic ear (M-O) were examined (see diagram below). P-CaMK-II colocalizes with acetylated tubulin in some cells and axons in a frontal view of the olfactory placode (D, arrow) and in spinal cord cell bodies (H), but is undetectable in spinal cord axons. P-CaMK-II localizes at the apical surface of pronephric ductal cells (K, arrowhead), at all surfaces of cloacal cells (L) and at the base of the hair cell kinocilium (O, P, arrows). Scale bars: 10 μm.

kidney becomes functional as early as 48 hpf and consists of the glomerulus, which empties into two pronephric ducts. These ducts connect at the cloaca for waste excretion (Drummond, 2005; Drummond et al., 1998). This simplified kidney nomenclature is used throughout this study, even though subregions have been recently characterized and named (Wingert et al., 2007). Within the pronephros, activated CaMK-II is first detected at 24 hpf in distal regions, and peaks at 30 hpf in both anterior and posterior regions of the pronephric ducts and cloacal cells (Fig. 3B). Activated CaMK-II persists until 72 hpf in the distal pronephric duct, cloaca and cloacal cilia. Although CaMK-II is expressed uniformly along the entire duct (Fig. 1I), CaMK-II activation is not uniform along the pronephros (Fig. 3B). In particular, a region of the pronephric duct in the distal half persistently lacks activated CaMK-II (Fig. 3B).

The subcellular location of activated CaMK-II provides additional insight into its role. P-CaMK-II is found associated with apical and basolateral cell surfaces and in intracellular clusters throughout the pronephros (Fig. 3C-E, arrowheads). Such activated CaMK-II clusters were previously reported in cells surrounding the KV (Francescatto et al., 2010) and have also been observed in brain tissue (Hudmon et al., 2005). P-CaMK-II is preferentially apical in proximal and distal ducts and more evenly distributed between apical and basolateral surfaces in the cloaca, colocalizing with plasma membranes in transgenic (CAAX:GFP) embryos (Fig. 3F-H). P-CaMK-II is found uniformly along the length of cloacal cilia (Fig. 3I-K), but is undetectable in ductal cilia in the same embryos (Fig. 3D), identifying the short (~3 μm) cloacal primary cilia as unique with respect to CaMK-II activation. Activated CaMK-II colocalizes with the α1 subunit of Na^+/K^+-ATPase, a marker for transporting epithelium (Liu et al., 2007), in basolateral focal sections (Fig. 3L-N), but is not exclusive to these cells.

Suppression of γ1 CaMK-II induces pronephric cyst formation

Although CaMK-II is encoded by four genes in mice and humans (*Camk2a*, *-2b*, *-2g*, *-2d*), it is encoded by seven transcriptionally active genes (*camk2a*, *-2b1*, *-2b2*, *-2g1*, *-2g2*, *-2d1*, *-2d2*) in zebrafish to generate over two dozen splice variants (Rothschild et al., 2009; Rothschild et al., 2007). Only γ1 CaMK-II was identified in the zebrafish kidney by using RT-PCR of isolated kidney cells or tissue (see Fig. S1A in the supplementary material). The γ1 CaMK-II splice variants expressed in the kidney ($\gamma1_C$ and $\gamma1_F$) are putative cytosolic variants as previously described (Rothschild et al., 2009; Rothschild et al., 2007). Whole-mount in situ hybridization detected transcripts of the *camk2g1* gene throughout the kidney all the way through to the cloaca (see Fig. S1B, arrow in the supplementary material) and in pronephric duct cells when counterstained with the acetylated tubulin antibody (see Fig. S1C in the supplementary material) or the *pax2* probe (see Fig. S1D-F in the supplementary material).

Furthermore, using previously validated gene-specific translation-blocking antisense MOs (Francescatto et al., 2010; Rothschild et al., 2009), only γ1 CaMK-II suppression interfered with pronephros development. This MO would suppress the expression of all γ1 splice variants. In particular, the injection of the *camk2g1* MO (1 ng) induced hydrocephaly and pronephric cysts, and destabilized cloacal cilia (Figs 4, 5). Hydrocephaly was observed as early as 48 hpf (Fig. 4B, arrow) and became more pronounced over time. Bilateral pronephric cysts were detected at the third somite, just posterior to the pectoral fins (Fig. 4D, arrow and inset) in whole embryos and in cross sections adjacent to the glomerulus (Fig. 4F, asterisks). Renal filtration assays (Fig. 4G-J) confirmed kidney defects in *camk2g1* morphants due to the persistence of Rhodamine-dextran (Fig. 4J) after pericardial injection.

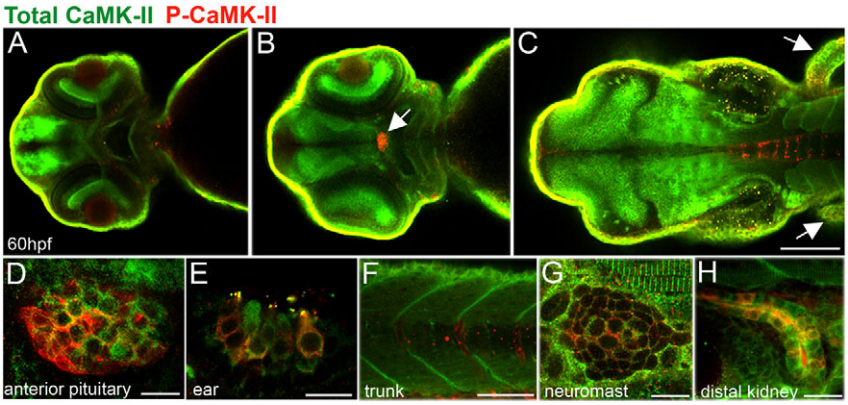

Fig. 2. Localization of activated and total CaMK-II in 60 hpf zebrafish embryos. (**A-D**) Dorsal views of zebrafish brain optical sections (from ventral to dorsal) showing CaMK-II in the forebrain (A), optic nerve and retina and the anterior pituitary (B, arrow, D) and, as expected, in the midbrain, hindbrain (C) and fins (C, arrows). As expected, total CaMK-II is found in the midbrain, hindbrain and fins. (**E-F**) Lateral views reveal P-CaMK-II in the hair cells of the ear (E), sarcomeres and somite boundaries (F,G), neuromasts (G) and kidney (H). Scale bars: in C, 10 μm for A,B; 10 μm in D,E,G,H; 100 μm in C; 50 μm in F.

Suppression of γ1 CaMK-II blocks anterior kidney convolution

Pronephric cysts have been correlated with defects in the collective anterior-directed migration of pronephric cells that form the convoluted proximal segment (Vasilyev et al., 2009). The hook-like convolution in the anterior region of the pronephros (Fig. 5A,C) is absent in *camk2g1* morphants (Fig. 5B,D). At 72 hpf, 87% of *camk2g1* morphant embryos (*n*=168) lacked the convolution. Defective convolution can be quantified by measuring the distance from the posterior edge of the ear to the anterior pronephric duct at 72 hpf (Vasilyev et al., 2009). MO suppression of *camk2g1* increased this distance from 140 μm in control embryos to 490 μm in morphant embryos (Fig. 5E).

Suppression of γ1 CaMK-II destabilizes cloacal cilia

The distal region of the pronephros is also susceptible to CaMK-II suppression. The distal pronephros exhibits gross (Fig. 5F,G) and kidney-specific (insets) morphogenic defects in *camk2g1* morphants at 72 hpf. These distal defects, which appeared as occlusions when examined one embryo at a time by through-focal microscopy, were observed in 73% of morphant embryos (*n*=143).

Since the disruption of cilia also induces kidney cysts in mouse and zebrafish embryos (Kramer-Zucker et al., 2005; Sullivan-Brown et al., 2008; Veland et al., 2009; Wilson, 2008), cilia were evaluated in *camk2g1* morphants. Ductal cilia formed and were motile in *camk2g1* morphants (Fig. 5H,I; see Movie 1 in the supplementary material). By contrast, cloacal cilia formed normally at 24 hpf in morphants, but then began to disassemble at 48 hpf (Fig. 5J,K) and by 72 hpf (Fig. 5L,M) had completely disassembled. Basal bodies persisted on the apical surface (Fig. 5M). Any remaining cloacal cilia in *camk2g1* morphants were immotile (see Movies 2 and 3 in the supplementary material). On average, thirteen cloacal cilia form at 72 hpf in control embryos, but less than one remains in *camk2g1* morphants (Fig. 5N). Of the remaining cloacal cilia, their length had decreased from 3 to 1.5 μm (Fig. 5O). These results point to a role for activated CaMK-II in stabilizing cloacal cilia.

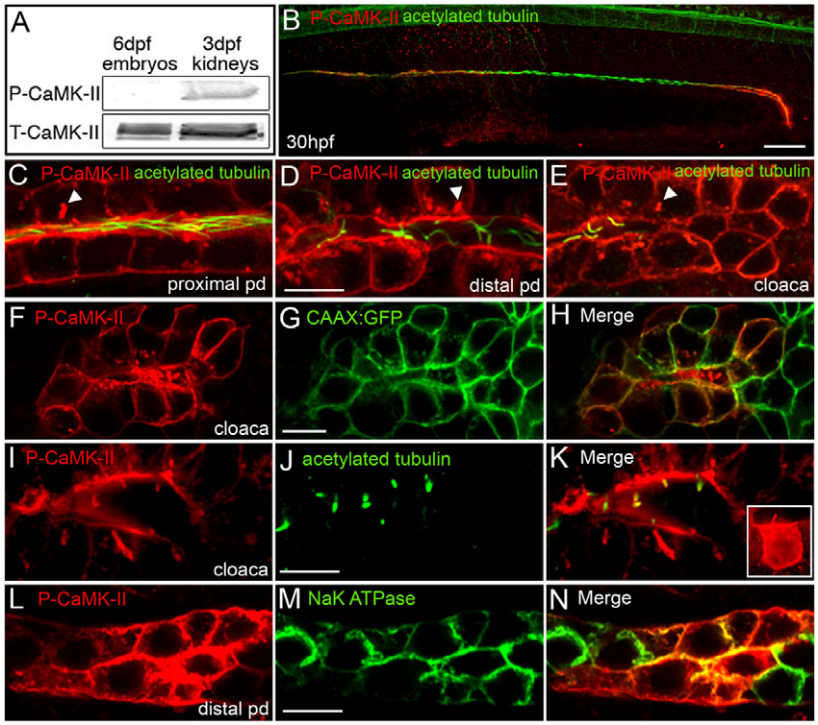

Fig. 3. Activated CaMK-II is enriched in the zebrafish pronephric kidney. (**A**) Immunoblot of P-CaMK-II and total CaMK-II in whole embryo (6 dpf) and isolated pronephric kidney (3 dpf) extracts demonstrates the preferential activation of CaMK-II in kidney cells. (**B-E**) P-CaMK-II localization in the anterior, posterior and cloacal cells of the pronephric duct at the lumenal focal plane as shown by counterstaining with acetylated tubulin. P-CaMK-II clusters are marked by arrowheads. (**F-H**) P-CaMK-II localization at the cell surface of cloacal cells and in cloacal cilia as shown by colocalization with the CAAX-GFP transgenic protein. (**I-K**) P-CaMK-II localizes at cloacal cilia (revealed by acetylated tubulin). The inset is a z-stack projection of P-CaMK-II in a single cloacal cell. (**L-N**) Basolateral focal sections of the distal pronephric duct reveals the colocalization of P-CaMK-II with the α1 subunit of the Na^+/K^+-ATPase at the surface of some but not all transporting epithelial cells. Scale bars: 50 μm in B; 10 μm in D,G,J,M.

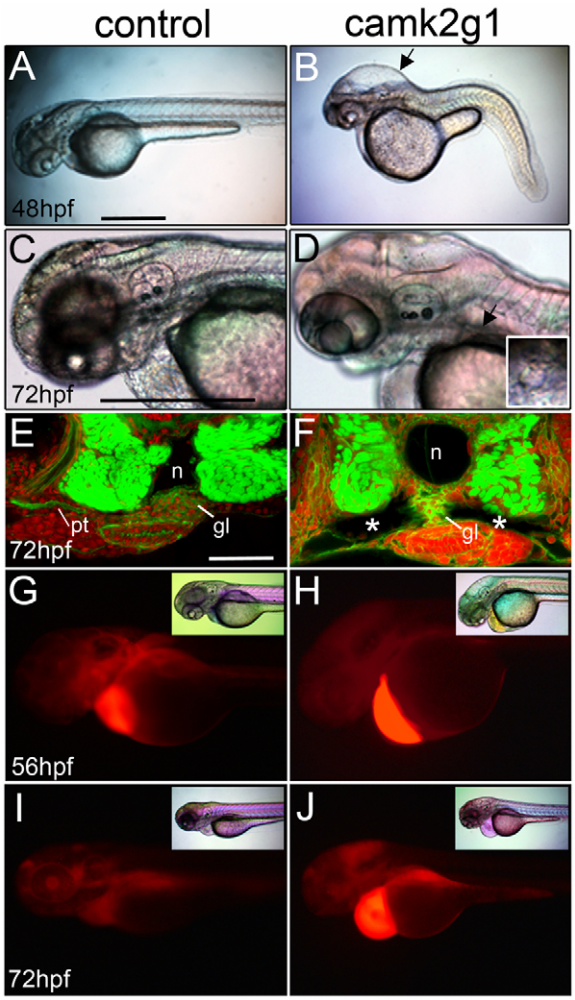

Fig. 4. Suppression of γ1 CaMK-II (*camk2g1*) induces cyst formation. (**A**,**B**) Lateral images of 48 hpf morphants injected with the *camk2g1* MO (1 ng) but not the control MO (1 ng) show hydrocephaly (arrow) and axis compression. (**C**,**D**) Hydrocephaly and cysts are visible at 72 hpf in *camk2g1* morphants (inset: dorsal view of anterior cyst (indicated by the arrow). (**E**,**F**) Cysts (*) in *camk2g1* morphants are revealed in vibratome sections stained with Alexa-Fluor-488-phalloidin and propidium iodide; pt, pronephric tubules; n, notochord; gl, glomerulus. (**G-J**) Renal filtration was observed in control embryos but not morphant embryos. Rhodamine-dextran was injected into the pericardial region at 56 hpf and then embryos were imaged with DIC optics (inset) or for fluorescence within 20 minutes (56 hpf) and then again at 72 hpf. Scale bars: 500 μm in A,C; 50 μm in E.

Since cystogenic morphants and mutants have been linked to alterations in cellular polarity, aPKC, γ-tubulin and F-actin were examined in *camk2g1* morphants but showed normal polarity (data not shown). Cystogenic morphants and mutants could also affect specification of important pronephric genes, but these were also unaffected in *camk2g1* morphants (Fig. 6). For instance, the expression of *pax2a* in intermediate mesoderm was unaltered at the 14-somite stage (Fig. 6A,B). At 24 hpf in both control and morphant embryos, *cdh17* demarcates the entire pronephric duct (Fig. 6C,D), whereas *gata3* and *ret1* appear in the distal regions (Fig. 6E-H). At 24 and 48 hpf, the anterior glomerular marker, *wt1a*, labels the podocyte precursor fields in both control and morphant embryos (Fig. 6I-L). The incomplete convergence of *wt1a* cells in *camk2g1* morphants at 48 hpf might also reflect morphogenic defects.

Kidney-targeted dominant-negative CaMK-II causes pronephric cystogenesis

Kidney development is also disrupted by a targeted dominant-negative CaMK-II mutant. The $K^{43}A$ point mutant lacks phosphotransferase activity, but can still hetero-oligomerize with endogenous CaMK-II and has previously been determined to act in a dominant-negative fashion (Francescatto et al., 2010). WT or dominant negative (DN) GFP-CaMK-II was targeted to pronephric cells. Embryos expressing DN, but not WT CaMK-II, developed pronephric cysts (Fig. 7C) and failed to undergo ductal convolution (Fig. 7F). Pronephric ducts that expressed DN, but not WT GFP-CaMK-II, were often shortened or branched at their anterior end (Fig. 7F,F′), suggestive of deficient or misdirected migration. Even though expression was mosaic (arrowheads), DN CaMK-II interfered with anterior convolution in a majority (76%; *n*=64) of embryos. However, neither distal pronephric duct development nor cloacal cilia beating were blocked (see Movie 4 in the supplementary material). The dominant inhibitory effect of this CaMK-II mutant on endogenous P-CaMK-II was seen in cells expressing DN, but not WT CaMK-II (Fig. 7G-L). For example, all five cells expressing GFP-DN CaMK-II in the field of view shown in Fig. 7J-L had diminished P-CaMK-II, whereas both WT cells had unaltered P-CaMK-II (Fig. 7G-I).

Activated CaMK-II is reduced in *pkd2* morphant embryos

CaMK-II can be activated by Ca^{2+} release from channels that are found in the endoplasmic reticulum, the plasma membrane or ciliary membrane, such as PKD2. The suppression of *pkd2*, a Ca^{2+}-conducting channel found in all these locations, causes a reduction of P-CaMK-II in cells surrounding the Kupffer's vesicle, leading to a loss of organ asymmetry (Francescatto et al., 2010). PKD2 is also expressed in the pronephros and *pkd2* morphants have cysts (Obara et al., 2006) that are similar in size and location to those observed in *camk2g1* morphants (Fig. 4F). As a result, we postulate that CaMK-II acts downstream of PKD2 during kidney development.

To determine if PKD2 Ca^{2+} activates CaMK-II, P-CaMK-II was assessed in *pkd2* morphants along the pronephric kidney in whole-mount embryos at 30 hpf (Fig. 8A-F) and in dissected 72 hpf pronephroi. In these morphants, P-CaMK-II at apical cell surfaces and at cytosolic clusters (Fig. 8C, arrowheads) was markedly reduced (Fig. 8D). Cloacal P-CaMK-II was reduced, but not eliminated, at both basolateral and apical surfaces (Fig. 8F), but completely eliminated from cilia (Fig. 8F, inset, asterisk). P-CaMK-II levels in other locations not linked to PKD2 function, such as the ear, forebrain and spinal cord cell bodies, was not diminished in *pkd2* morphants (data not shown).

A second method to evaluate whether activated kidney CaMK-II is dependent on PKD2 is through CaMK-II activity assays conducted in the presence and absence of Ca^{2+}, as previously described (Francescatto et al., 2010). Prolonged Ca^{2+} stimulation leads to autophosphorylation (P-CaMK-II), yielding an enzyme that is active in the absence of Ca^{2+}. The percentage of Ca^{2+}-dependent activity that is Ca^{2+} independent (autonomous) can be determined from cell lysates and kinase assays; this 'autonomy' rarely exceeds ~50%. CaMK-II autonomy was determined in lysates prepared from excised pronephric ducts from control (Fig. 8G,H) and *pkd2* morphant (not shown) embryos. Isolated kidneys contain some non-kidney cells, but are enriched in P-CaMK-II (Fig. 3A). CaMK-II autonomy was approximately 37% in control embryos and 23% in *pkd2* morphant

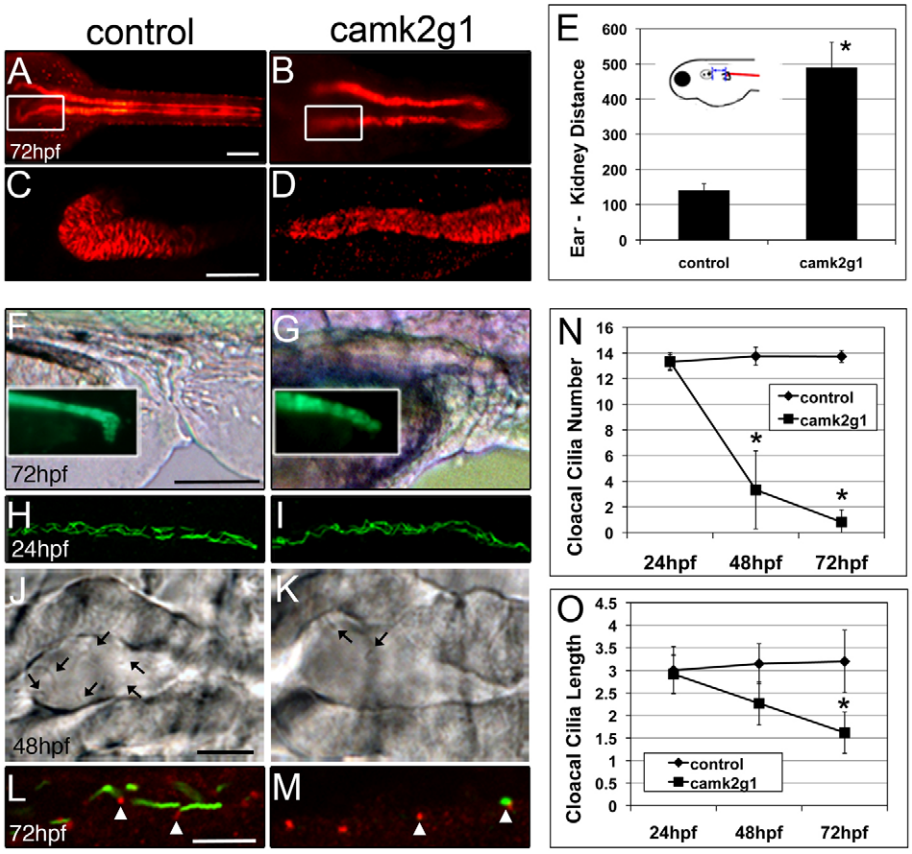

Fig. 5. Suppression of γ1 CaMK-II (*camk2g1*) by injection of the *camk2g1* MO (1ng) induces anterior and posterior kidney defects. (**A**,**B**) Dorsal view of entire pronephric ducts immunostained for α1 Na^+/K^+-ATPase; (**C**,**D**) regions outlined by white boxes are shown in z-stack projections. (**E**) Anterior migration is blocked in *camk2g1* morphants as inferred from the increase in the distance between the anterior kidney and posterior ear. (**F**,**G**) Morphogenic alterations in the ductal region of the pronephros are evident using both DIC optics and GFP-α1 Na^+/K^+-ATPase fluorescence (insets). (**H**,**I**) Pronephric ductal cilia appear normal at all time points as shown by acetylated tubulin immunostaining at 24 hpf. (**J**,**K**) DIC images of the cloaca at 48 hpf. Arrows indicate cilia. (**L**,**M**) Acetylated tubulin (green) and γ-tubulin (red) show a loss of cloacal cilia but a retention of the basal body (arrowheads) in morphants. (**N**,**O**) Cloacal cilia number and length (of remaining cilia) were measured at 24, 48 and 72 hpf. *P<0.005. Scale bars: 100 μm in A,C,F; 5 μm in J,L.

embryos, thus demonstrating a significant, but not complete reduction (~40%) in CaMK-II autonomy (Fig. 8I). These results indicate that the high levels of activated CaMK-II in the zebrafish kidney are due in large part to PKD2 Ca^{2+}.

Ectopic expression of CaMK-II rescues cyst development in *pkd2* morphants

Further evidence that CaMK-II acts downstream of PKD2 was obtained by rescuing *pkd2* morphants with a constitutively active phosphomimetic ($T^{287}D$) CaMK-II mutant (Fig. 9). The *pkd2* MO was injected alone or with GFP-tagged $T^{287}D$ δ_E CaMK-II, as previously described (Rothschild et al., 2009). Like *camk2g1* morphants, over 90% of *pkd2* morphants exhibited hydrocephaly, tail curvature (Fig. 9B), pronephric occlusion (Fig. 9E), and lacked convolution (Fig. 9H,H′). When embryos were injected with $T^{287}D$, but not when injected with WT CaMK-II, tail curvature and hydrocephaly were reduced (Fig. 9C) and pronephric occlusions (Fig. 9F) decreased from 96% to 52% (n=213) of embryos. Convolution defects were reduced from 91% (n=187) in *pkd2* morphants to 52% (n=189) in morphants expressing $T^{287}D$ CaMK-II. Like DN CaMK-II (Fig. 7), ectopic $T^{287}D$ CaMK-II was enriched apically in pronephric epithelial cells (Fig. 9J,L), whereas Na^+/K^+-ATPase is more basolateral in the same cells. The ability of $T^{287}D$ CaMK-II to rescue both the posterior and the anterior defects of *pkd2* morphant embryos was found to be statistically significant (Fig. 9M,N).

As seen with *camk2g1* morphants, *pkd2* morphants have cloacal cilia that become unstable during the second day of development (Fig. 9O-R). At 72 hpf, *pkd2* morphants retained only 2.5 cilia, with an average length of 1.5 μm (Fig. 9O,P), whereas basal bodies persisted apically (Fig. 9Q,R). Similar to *camk2g1* morphants, 83% of *pkd2* morphants exhibited defective or no cloacal cilia beating (see Movie 5 in the supplementary material). Ciliary defects in *pkd2* morphants could not be recovered with ectopic $T^{287}D$ CaMK-II, perhaps for the same reason that DN CaMK-II was incapable of inducing cloacal cilia defects. Ciliary instability was not observed in ductal cilia, indicating a special, yet undefined role for PKD2, Ca^{2+} and CaMK-II in cloacal cilia stability.

Synergistic relationship between camk2g1 and pkd2 in cystic development

A linkage between PKD2 and CaMK-II was also demonstrated by co-injecting embryos with sub-effective doses of MOs (Fig. 10A-C). Such synergistic approaches using pairs of MOs have been previously used to link separate components in the same genetic pathway (Mably et al., 2006). Injection of one-quarter of the normal amount of *pkd2* or *camk2g1* MOs alone did not alter anterior pronephric development, as assessed by both morphology (Fig. 10D-F) and ear-kidney distance (Fig. 10H). However, the co-injection of these same sub-effective *pkd2* and *camk2g1* MO amounts inhibited convolution in 66% (n=74) of embryos (Fig. 10D-G) and reduced anterior migration (Fig. 10H) to the same extent as the higher levels of either MO alone (Figs 5, 9). Although occlusions were not evident in *pkd2/camk2g1* co-morphants (Fig. 10G), cloacal cilia were destabilized (Fig. 10I-M) and beat improperly in 85% of injected embryos (see Movies 6-8 in the supplementary material). The findings from this study collectively demonstrate the relationship between PKD2 and CaMK-II in the developing zebrafish kidney and their role in cloacal cilia stability and proper pronephric morphogenesis.

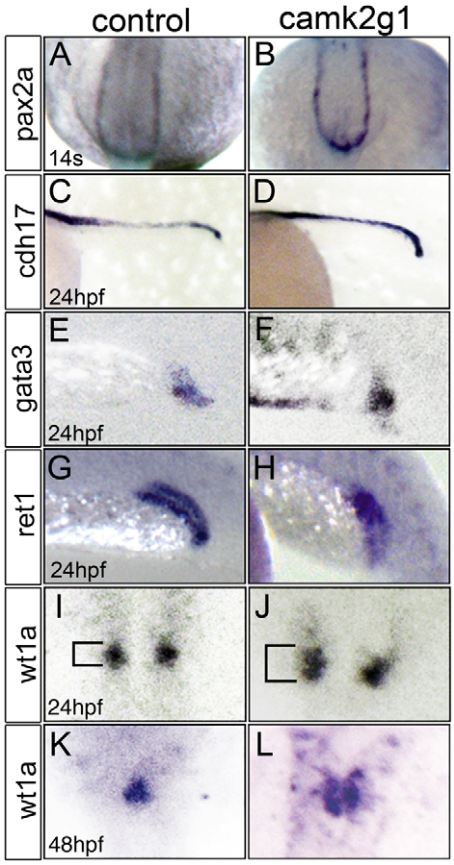

Fig. 6. Pronephros specification in *camk2g1* morphants. Whole mount in situ hybridization of control and *camk2g1* morphants using (**A**,**B**) *pax2a* at 14 somites (dorsal view), (**C**,**D**) *cdh17,* (**E**,**F**) *gata3,* (**G**,**H**) *ret1* at 24 hpf (C-H, lateral view, anterior to the left); (**I-L**) *wt1a* at 24 hpf and 48 hpf (dorsal views).

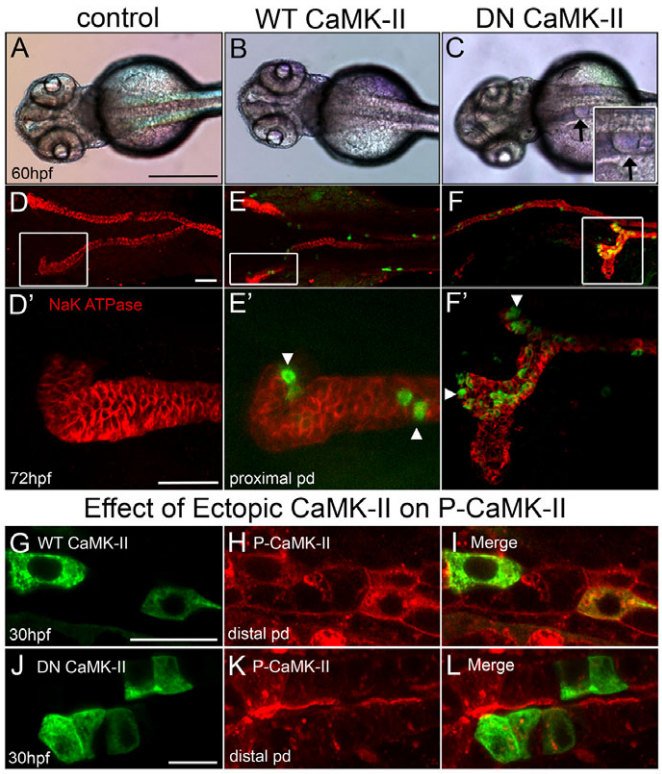

Fig. 7. Dominant-negative CaMK-II phenocopies *camk2g1* morphants. (**A-C**) Dorsal views of 60 hpf embryos that were uninjected (control) or injected with kidney-targeted wild-type (WT) and dominant negative (DN) GFP-CaMK-II. Cysts are evident in DN CaMK-II embryos as shown in the inset (arrows). (**D-F**) Control and WT embryos immunostained for α1 Na^+/K^+-ATPase undergo proper convolution but DN embryos fail to convolute in proportion to expression (GFP). (**D′-F′**) Z-stack renderings of the anterior pronephric duct regions outlined by white boxes in D-F. (**G-L**) Kidney-targeted WT and DN CaMK-II are expressed in pronephric cells, but only DN CaMK-II diminishes P-CaMK-II. Scale bars: 500 μm in A; 20 μm in D,D′; 10 μm in G,J.

DISCUSSION

We conclude that the Ca^{2+}/CaM-dependent protein kinase, CaMK-II, is an essential effector of the Ca^{2+} channel, PKD2, in the developing pronephros. We have reached this conclusion based on multiple lines of evidence. First, CaMK-II deficiencies caused by either CaMK-II translation-blocking MOs or dominant-negative constructs phenocopy *pkd2* morphants. Second, *pkd2* morphants have reduced levels of activated (autophosphorylated) CaMK-II. Third, constitutively active CaMK-II can rescue *pkd2* morphants. Finally, CaMK-II and PKD2 suppression work synergistically, thus supporting their placement in the same genetic pathway. Our findings suggest that CaMK-II promotes pronephric development by enabling both anterior migration and posterior morphogenesis, including ciliary stability. This is the first report of a direct downstream Ca^{2+}-dependent target of PKD2 in the kidney and is consistent with the finding that CaMK-II is activated by PKD2 in ciliated cells of the zebrafish KV (Francescatto et al., 2010).

Activated CaMK-II has now been detected in multiple ciliated tissues during development including the KV, the inner ear and neuromasts. These sites of CaMK-II activation are consistent with known locations of prolonged Ca^{2+} elevation in embryos of zebrafish and other species (Webb and Miller, 2003; Webb and Miller, 2007). These locations are also consistent with tissues that exhibit morphogenic defects after CaMK-II suppression (Francescatto et al., 2010; Rothschild et al., 2009). Many of these tissues express PKD2 (Obara et al., 2006), but other Ca^{2+} channels, such as the RyR, are also known to be required for full CaMK-II activation (Francescatto et al., 2010). This suggests that CaMK-II integrates Ca^{2+} signals from more than a single source and is consistent with the inability to completely inactivate pronephric CaMK-II in PKD2-deficient embryos.

There are many ways in which CaMK-II could enable development and function of ciliated tissues. In the kidney, anterior and posterior regions can be considered separately, but are interdependent. Zebrafish pronephros development requires anterior migration of the proximal pronephric epithelia to form pronephric tubules that link to the glomerulus and form the embryonic kidney. Collective migration of duct cells begins at 28.5 hpf, coincident with highly active CaMK-II in the proximal pronephric duct, where pronephric epithelial cells undergo a proximally directed migration toward the glomerulus. This migration occurs as a sheet, where apical cell connections are maintained and basal surfaces project lamellipodia at the leading edge. Pronephric migratory cells require dynamic adhesions to the basement membrane and focal adhesion turnover (Vasilyev et al., 2009). The inactivation of focal-adhesion proteins leads to the

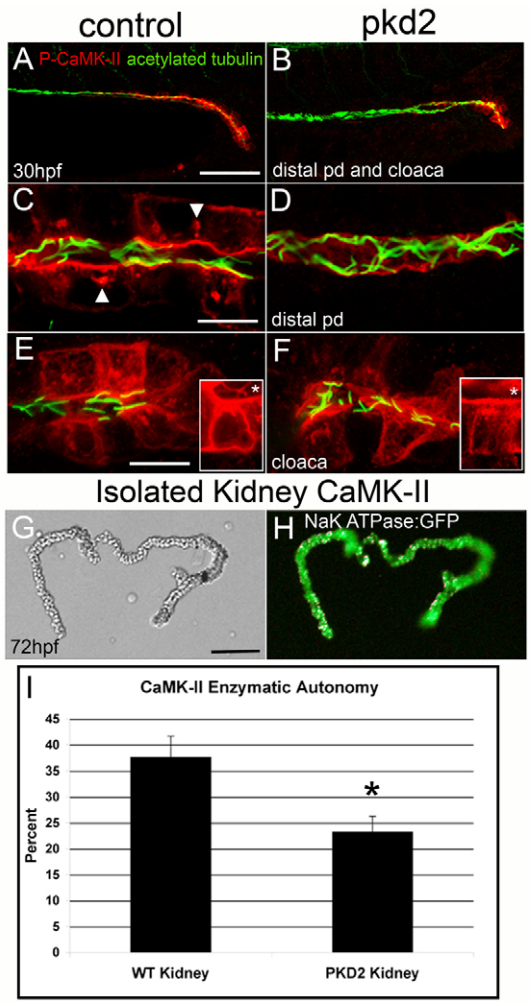

Fig. 8. Active CaMK-II is reduced in *pkd2* morphants. (**A**,**C**,**E**) Control and (**B**,**D**,**F**) *pkd2* morphants were fixed at 30 hpf and immunolabeled with P-CaMK-II and counterstained for acetylated tubulin. (A,B) P-CaMK-II is reduced in both the distal pronephric duct and cloaca in the morphant. (C) High-magnification image of the distal pronephric duct identifies activated CaMK-II at the apical and basolateral surfaces and in clusters (arrowheads). (D) Activated CaMK-II is lost or greatly diminished in *pkd2* morphants. (E,F) P-CaMK-II is reduced, but not absent from cloacal cells in F, but completely lost from cloacal cilia, which are present and normally exhibit activated CaMK-II (inset,*). The insets are z-stack projections of a single cloacal cell stained only with P-CaMK-II. (**G**,**H**) Pronephric ducts were dissected from α1 Na^+/K^+-ATPase-GFP transgenic embryos at 72 hpf. (G) DIC and (H) fluorescence images. (**I**) CaMK-II enzymatic assay of isolated 3 dpf kidneys shows the reduction, but not elimination of CaMK-II enzymatic autonomy in *pkd2* morphants. *P<0.005. Scale bars: 50 μm in A,G; 10 μm in C,E.

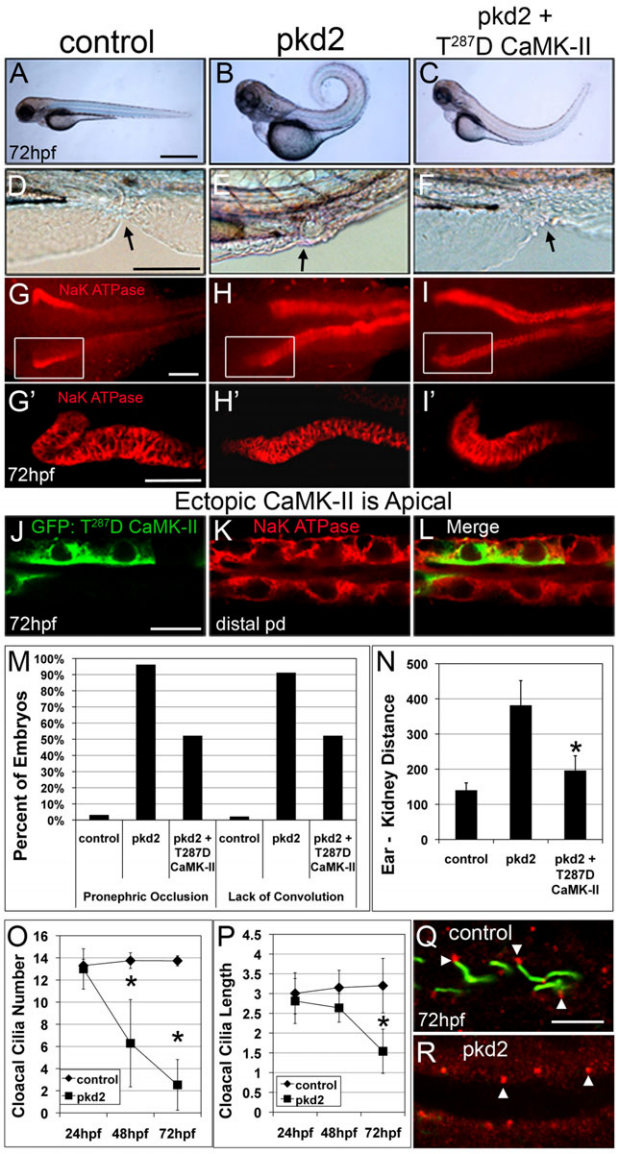

Fig. 9. Constitutively active ($T^{287}D$) CaMK-II reverses pronephric developmental defects. (**A-F**) Lateral views of 72 hpf entire embryos (A-C) and the cloaca (D-F; arrows indicate the end of the cloaca) after injection of *pkd2* MO (4 ng) with or without $T^{287}D$ CaMK-II cDNA (30 pg). (**G-I**) Immunostaining α1 Na^+/K^+-ATPase identifies the pronephric ducts. (**G′-I′**) Z-stack renderings of the regions outlined by white boxes in G-I. (**J-L**) $T^{287}D$ CaMK-II localizes to apical surfaces of pronephric epithelial cells. (**M**) Quantification of the reversal of the *pkd2* morphant phenotype (posterior: occlusion and anterior: convolution) by $T^{287}D$ CaMK-II (n=125-268). (**N**) Recovery of anterior migration of pronephric epithelial cells by ectopic $T^{287}D$ CaMK-II in *pkd2* morphants as assessed by a decrease in posterior ear-anterior kidney distance (in μm; n=50-60). (**O**,**P**) Cloacal cilia number and length were determined at 24, 48 and 72 hpf. *P<0.005. (**Q**,**R**) Cloacal cilia disassemble but basal bodies remain apical as assessed by co-staining with acetylated tubulin (green) and γ-tubulin (red) at 72 hpf. Scale bars: 500 μm in A; 100 μm in D; 20 μm in G,G′; 10 μm in J; 5 μm in Q.

development of cysts in mice (Lo et al., 1997). Suppression of *camk2g1* and *pkd2* inhibited proper pronephric duct migration and anterior convolution, whereas *pkd2* morphants, ectopically expressing constitutively active CaMK-II, partially recovered cellular migration.

Both CaMK-II and PKD1 have been identified at focal adhesions and have been independently linked to focal adhesion turnover (Easley et al., 2008; Wilson et al., 1999). PKD1 interacts with the extracellular matrix (ECM) and focal adhesion proteins (Wilson, 2004). Cells from ADPKD patients with mutations in

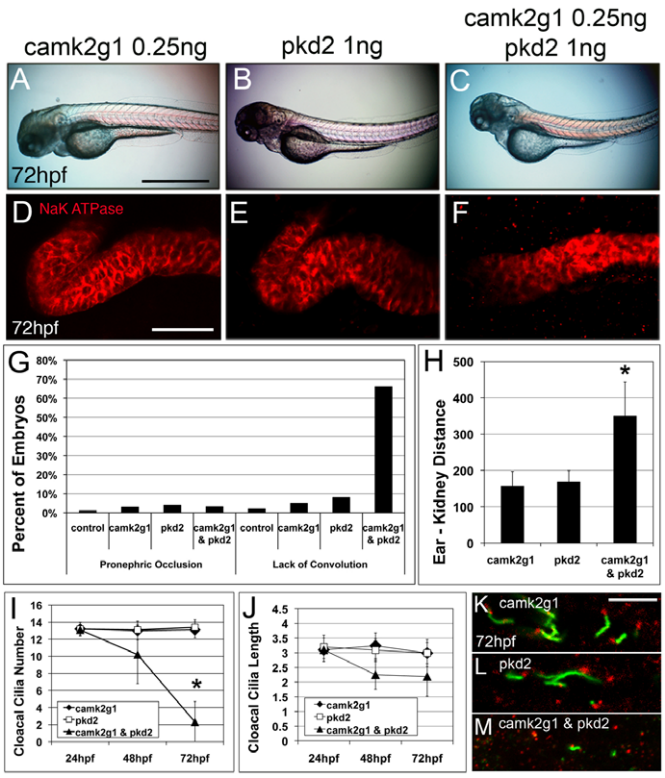

Fig. 10. CaMK-II and PKD2 act in the same molecular pathway. (**A-F**) Embryos injected with *camk2g1* MO (0.25 ng), *pkd2* MO (1 ng) or *camk2g1* and *pkd2* MOs (0.25 ng and 1 ng, respectively) were imaged at 72 hpf from lateral perspectives using DIC optics (A-C) or dorsal perspectives using immunofluorescence microscopy to identify α1 Na^+/K^+-ATPase (D-F). (**G**,**H**) Pronephric occlusions and convolution at 72 hpf (G; *n*=80-125) and pronephric migration as assessed by posterior ear-anterior kidney distance in μm at 72 hpf (H; *n*=60-82). (**I**,**J**) Cloacal cilia number (I) and cilia length (J) were determined at 24, 48 and 72 hpf. **P*<0.005. (**K-M**) 72 hpf morphants immunolabeled with acetylated tubulin (green) and γ–tubulin (red) show a loss of cloacal cilia but retention of the basal body. Scale bars: 500 μm in A; 20 μm in D; 5 μm in K.

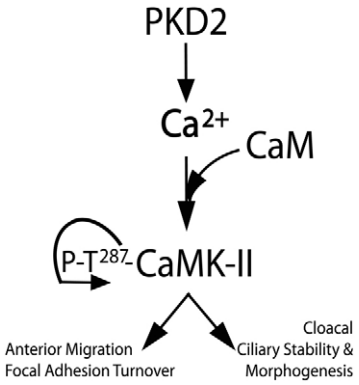

Fig. 11. Model of CaMK-II activation and multifunctionality in the developing zebrafish kidney.

PKD1 exhibit increased adhesiveness to the extracellular matrix and decreased motility (Wilson et al., 1999). This phenotype is identical to that observed when CaMK-II is acutely inhibited in mouse fibroblasts (Easley et al., 2008). Focal adhesion turnover requires the dephosphorylation of tyrosine residues on paxillin and FAK (Mitra et al., 2005). PKD1 colocalizes with paxillin in renal cell culture, suggesting a possible link between PKD1 and CaMK-II at focal adhesions (Israeli et al., 2010; Wilson, 2001). Therefore, the lack of migration in anterior pronephric cells in *pkd2* and *camk2g1* morphants could be due to the inhibition of CaMK-II at focal adhesions.

Cloacal cells undergo shape changes, exhibit apicobasal polarity and depend on migratory morphogenesis (Pyati et al., 2006; Slanchev et al., 2011; Vasilyev et al., 2009), but unlike proximal epithelial cells, do not migrate as collectives (Vasilyev et al., 2009). Activated CaMK-II is enriched at the apical surface of ductal cells and is known to directly interact with and stabilize F-actin (Easley et al., 2006; Lin and Redmond, 2008; Okamoto et al., 2007; Sanabria et al., 2009). Apical constriction mediated by actinomyosin is necessary for the alterations in cell shape that lead to proper tissue development (Daggett et al., 2007), including duct formation (Sawyer et al., 2010) and could explain a role for CaMK-II in cloacal cells.

This study has also provided some insight into the role of Ca^{2+} signaling in ciliary stability. Our findings indicate that the PKD2-dependent activation of CaMK-II is necessary to maintain primary cilia in the cloacal region. CaMK-II is activated along the entire length of these cilia and when inactivated destabilizes cilia. Activated CaMK-II might stabilize cilia through its inhibition of the microtubule destabilizing protein, kinesin-13 (MCAK) (Holmfeldt et al., 2005; Piao et al., 2009). Interestingly, cilium assembly is dependent on the Polo kinase, Plk4, acting on CEP 152 (Cizmecioglu et al., 2010; Hatch et al., 2010). CaMK-II is known to collaborate with the Plx1 Polo kinase to promote meiotic resumption (Liu and Maller, 2005).

Although the loss of cloacal cilia or the presence of ductal occlusions can cause improper anteriorly directed pronephric epithelial migration and cyst development, independently blocking anterior kidney development, as observed with the DN CaMK-II, can induce cysts without a loss of cilia. A loss of fluid flow is also seen when either ductal cilia fail to assemble or in morphants where blood flow is inhibited (Vasilyev et al., 2009). These separate, but inter-related, anterior and posterior morphogenic events are paralleled by the anterior and posterior activation of CaMK-II.

There is a significant amount of overlap between known CaMK-II substrates or binding partners and those implicated in kidney development or cystic disease. For example, histone deacetylases (HDACs) are known CaMK-II targets and have become a viable therapeutic target in treating PKD. CaMK-II is known to phosphorylate HDAC4 or HDAC5 at conserved residues (Backs et al., 2008; Zhang et al., 2007), leading to cytosolic HDAC retention and thus the upregulation of MEF2C target genes (Little et al., 2007; Zhang et al., 2007). One of these MEF2C target genes is missing in metastasis (*Mim*; *Mtss1* – Mouse Genome Informatics), which is necessary for ciliogenesis (Bershteyn et al., 2010) and actin cytoskeletal organization (Saarikangas et al., 2011). *Mef2c* knockout mice and MIM-deficient mice develop tubule dilations and cysts, whereas inhibition of HDAC5 in *Pkd2*$^{-/-}$ mice suppresses renal cyst formation (Xia et al., 2010). In zebrafish, HDAC inhibition reverses cystogenesis in *pkd2* morphants (Cao et al., 2009). A plausible mechanism to partially explain kidney development and homeostasis would depend on the activation of

CaMK-II by PKD2 Ca^{2+}, which then leads to the phosphorylation and cytosolic retention of HDAC4 and/or HDAC5 and sustained *mef2c* gene expression.

In summary, our results are consistent with PKD2-dependent Ca^{2+} elevations, which activate CaMK-II. Activated CaMK-II could then balance apical polarity and constriction, cell migration, ciliary function and gene expression as the kidney forms, functions and grows (Fig. 11). Cysts are the result of mutations in components of this pathway at any location to cause incomplete ductal-glomerular connections, pronephric occlusions and cloacal ciliary disassembly. These findings have identified CaMK-II as a previously missing link in this pathway and raise the possibility that CaMK-II and its targets might be novel therapeutic targets for ADPKD and other ciliopathies.

Acknowledgements
The authors gratefully acknowledge Jamie Lahvic, Bennett Childs, Jamie McLeod, Alexandra Myers and Amritha Yelamilli for their assistance with this study; and Becky Burdine, Alan Davidson, Amanda Dickinson, James Lister, Lila Solnica-Krezel and Joe Yost for sharing useful reagents and advice. Supported by National Science Foundation grant IOS-0817658.

Competing interests statement
The authors declare no competing financial interests.

Supplementary material
Supplementary material for this article is available at
http://dev.biologists.org/lookup/suppl/doi:10.1242/dev.066340/-/DC1

References
Backs, J., Backs, T., Bezprozvannaya, S., McKinsey, T. A. and Olson, E. N. (2008). Histone deacetylase 4 confers CaM kinase II responsiveness to histone deacetylase 5 by oligomerization. *Mol. Cell. Biol.* **28**, 3437-3445.
Bershteyn, M., Atwood, S. X., Woo, W. M., Li, M. and Oro, A. E. (2010). MIM and cortactin antagonism regulates ciliogenesis and hedgehog signaling. *Dev. Cell* **19**, 270-283.
Bisgrove, B. W., Snarr, B. S., Emrazian, A. and Yost, H. J. (2005). Polaris and Polycystin-2 in dorsal forerunner cells and Kupffer's vesicle are required for specification of the zebrafish left-right axis. *Dev. Biol.* **287**, 274-288.
Cai, Y., Maeda, Y., Cedzich, A., Torres, V. E., Wu, G., Hayashi, T., Mochizuki, T., Park, J. H., Witzgall, R. and Somlo, S. (1999). Identification and characterization of polycystin-2, the PKD2 gene product. *J. Biol. Chem.* **274**, 28557-28565.
Cao, Y., Semanchik, N., Lee, S. H., Somlo, S., Barbano, P. E., Coifman, R. and Sun, Z. (2009). Chemical modifier screen identifies HDAC inhibitors as suppressors of PKD models. *Proc. Natl. Acad. Sci. USA* **106**, 21819-21824.
Casuscelli, J., Schmidt, S., DeGray, B., Petri, E. T., Celic, A., Folta-Stogniew, E., Ehrlich, B. E. and Boggon, T. J. (2009). Analysis of the cytoplasmic interaction between polycystin-1 and polycystin-2. *Am. J. Physiol. Renal Physiol.* **297**, F1310-F1315.
Cizmecioglu, O., Arnold, M., Bahtz, R., Settele, F., Ehret, L., Haselmann-Weiss, U., Antony, C. and Hoffmann, I. (2010). Cep152 acts as a scaffold for recruitment of Plk4 and CPAP to the centrosome. *J. Cell Biol.* **191**, 731-739.
Clapham, D. E. (2003). TRP channels as cellular sensors. *Nature* **426**, 517-524.
Daggett, D. F., Domingo, C. R., Currie, P. D. and Amacher, S. L. (2007). Control of morphogenetic cell movements in the early zebrafish myotome. *Dev. Biol.* **309**, 169-179.
Drummond, I. A. (2005). Kidney development and disease in the zebrafish. *J. Am. Soc. Nephrol.* **16**, 299-304.
Drummond, I. A., Majumdar, A., Hentschel, H., Elger, M., Solnica-Krezel, L., Schier, A. F., Neuhauss, S. C., Stemple, D. L., Zwartkruis, F., Rangini, Z. et al. (1998). Early development of the zebrafish pronephros and analysis of mutations affecting pronephric function. *Development* **125**, 4655-4667.
Easley, C. A., Faison, M. O., Kirsch, T. L., Lee, J. A., Seward, M. E. and Tombes, R. M. (2006). Laminin activates CaMK-II to stabilize nascent embryonic axons. *Brain Res.* **1092**, 59-68.
Easley, C. A., Brown, C. M., Horwitz, A. F. and Tombes, R. M. (2008). CaMK-II promotes focal adhesion turnover and cell motility by inducing tyrosine dephosphorylation of FAK and paxillin. *Cell Motil. Cytoskeleton* **65**, 662-674.
Feng, S., Okenka, G. M., Bai, C. X., Streets, A. J., Newby, L. J., DeChant, B. T., Tsiokas, L., Obara, T. and Ong, A. C. (2008). Identification and functional characterization of an N-terminal oligomerization domain for polycystin-2. *J. Biol. Chem.* **283**, 28471-28479.
Fliegauf, M., Benzing, T. and Omran, H. (2007). When cilia go bad: cilia defects and ciliopathies. *Nat. Rev. Mol. Cell Biol.* **8**, 880-893.
Francescatto, L., Rothschild, S. C., Myers, A. L. and Tombes, R. M. (2010). The activation of membrane targeted CaMK-II in the zebrafish Kupffer's vesicle is required for left-right asymmetry. *Development* **137**, 2753-2762.
Gallagher, A. R., Hoffmann, S., Brown, N., Cedzich, A., Meruvu, S., Podlich, D., Feng, Y., Konecke, V., de Vries, U., Hammes, H. P. et al. (2006). A truncated polycystin-2 protein causes polycystic kidney disease and retinal degeneration in transgenic rats. *J. Am. Soc. Nephrol.* **17**, 2719-2730.
Gattone, V. H., 2nd, Chen, N. X., Sinders, R. M., Seifert, M. F., Duan, D., Martin, D., Henley, C. and Moe, S. M. (2009). Calcimimetic inhibits late-stage cyst growth in ADPKD. *J. Am. Soc. Nephrol.* **20**, 1527-1532.
Giamarchi, A., Feng, S., Rodat-Despoix, L., Xu, Y., Bubenshchikova, E., Newby, L. J., Hao, J., Gaudioso, C., Crest, M., Lupas, A. N. et al. (2010). A polycystin-2 (TRPP2) dimerization domain essential for the function of heteromeric polycystin complexes. *EMBO J.* **29**, 1176-1191.
Hanaoka, K., Qian, F., Boletta, A., Bhunia, A. K., Piontek, K., Tsiokas, L., Sukhatme, V. P., Guggino, W. B. and Germino, G. G. (2000). Co-assembly of polycystin-1 and -2 produces unique cation-permeable currents. *Nature* **408**, 990-994.
Hatch, E. M., Kulukian, A., Holland, A. J., Cleveland, D. W. and Stearns, T. (2010). Cep152 interacts with Plk4 and is required for centriole duplication. *J. Cell Biol.* **191**, 721-729.
Holmfeldt, P., Zhang, X., Stenmark, S., Walczak, C. E. and Gullberg, M. (2005). CaMKIIgamma-mediated inactivation of the Kin I kinesin MCAK is essential for bipolar spindle formation. *EMBO J.* **24**, 1256-1266.
Hudmon, A. and Schulman, H. (2002). Neuronal Ca^{2+}/calmodulin-dependent protein kinase II: the role of structure and autoregulation in cellular function. *Annu. Rev. Biochem.* **71**, 473-510.
Hudmon, A., Lebel, E., Roy, H., Sik, A., Schulman, H., Waxham, M. N. and De Koninck, P. (2005). A mechanism for Ca^{2+}/calmodulin-dependent protein kinase II clustering at synaptic and nonsynaptic sites based on self-association. *J. Neurosci.* **25**, 6971-6983.
Israeli, S., Amsler, K., Zheleznova, N. and Wilson, P. D. (2010). Abnormalities in focal adhesion complex formation, regulation, and function in human autosomal recessive polycystic kidney disease epithelial cells. *Am. J. Physiol. Cell Physiol.* **298**, C831-C846.
Kimmel, C. B., Ballard, W. W., Kimmel, S. R., Ullmann, B. and Schilling, T. F. (1995). Stages of embryonic development of the zebrafish. *Dev. Dyn.* **203**, 253-310.
Kramer-Zucker, A. G., Olale, F., Haycraft, C. J., Yoder, B. K., Schier, A. F. and Drummond, I. A. (2005). Cilia-driven fluid flow in the zebrafish pronephros, brain and Kupffer's vesicle is required for normal organogenesis. *Development* **132**, 1907-1921.
Kühl, M., Sheldahl, L., Malbon, C. C. and Moon, R. T. (2000). Ca^{2+}/calmodulin-dependent protein kinase II is stimulated by Wnt and Frizzled homologs and promotes ventral cell fates in Xenopus. *J. Biol. Chem.* **275**, 12701-12711.
Lancaster, M. A. and Gleeson, J. G. (2009). The primary cilium as a cellular signaling center: lessons from disease. *Curr. Opin. Genet. Dev.* **19**, 220-229.
Lin, Y. C. and Redmond, L. (2008). CaMKIIbeta binding to stable F-actin in vivo regulates F-actin filament stability. *Proc. Natl. Acad. Sci. USA* **105**, 15791-15796.
Little, G. H., Bai, Y., Williams, T. and Poizat, C. (2007). Nuclear calcium/calmodulin-dependent protein kinase IIdelta preferentially transmits signals to histone deacetylase 4 in cardiac cells. *J. Biol. Chem.* **282**, 7219-7231.
Liu, J. and Maller, J. L. (2005). Calcium elevation at fertilization coordinates phosphorylation of XErp1/Emi2 by Plx1 and CaMK II to release metaphase arrest by cytostatic factor. *Curr. Biol.* **15**, 1458-1468.
Liu, Y., Pathak, N., Kramer-Zucker, A. and Drummond, I. A. (2007). Notch signaling controls the differentiation of transporting epithelia and multiciliated cells in the zebrafish pronephros. *Development* **134**, 1111-1122.
Lo, S. H., Yu, Q. C., Degenstein, L., Chen, L. B. and Fuchs, E. (1997). Progressive kidney degeneration in mice lacking tensin. *J. Cell Biol.* **136**, 1349-1361.
Mably, J. D., Chuang, L. P., Serluca, F. C., Mohideen, M. A., Chen, J. N. and Fishman, M. C. (2006). *santa* and *valentine* pattern concentric growth of cardiac myocardium in the zebrafish. *Development* **133**, 3139-3146.
Mitra, S. K., Hanson, D. A. and Schlaepfer, D. D. (2005). Focal adhesion kinase: in command and control of cell motility. *Nat. Rev. Mol. Cell Biol.* **6**, 56-68.
Nagao, S., Nishii, K., Yoshihara, D., Kurahashi, H., Nagaoka, K., Yamashita, T., Takahashi, H., Yamaguchi, T., Calvet, J. P. and Wallace, D. P. (2008). Calcium channel inhibition accelerates polycystic kidney disease progression in the Cy/+ rat. *Kidney Int.* **73**, 269-277.
Obara, T., Mangos, S., Liu, Y., Zhao, J., Wiessner, S., Kramer-Zucker, A. G., Olale, F., Schier, A. F. and Drummond, I. A. (2006). Polycystin-2 immunolocalization and function in zebrafish. *J. Am. Soc. Nephrol.* **17**, 2706-2718.
Okamoto, K., Narayanan, R., Lee, S. H., Murata, K. and Hayashi, Y. (2007). The role of CaMKII as an F-actin-bundling protein crucial for maintenance of dendritic spine structure. *Proc. Natl. Acad. Sci. USA* **104**, 6418-6423.
Pennekamp, P., Karcher, C., Fischer, A., Schweickert, A., Skryabin, B., Horst, J., Blum, M. and Dworniczak, B. (2002). The ion channel polycystin-2 is required for left-right axis determination in mice. *Curr. Biol.* **12**, 938-943.

Piao, T., Luo, M., Wang, L., Guo, Y., Li, D., Li, P., Snell, W. J. and Pan, J. (2009). A microtubule depolymerizing kinesin functions during both flagellar disassembly and flagellar assembly in Chlamydomonas. *Proc. Natl. Acad. Sci. USA* **106**, 4713-4718.
Porter, G. A., Jr, Makuck, R. F. and Rivkees, S. A. (2003). Intracellular calcium plays an essential role in cardiac development. *Dev. Dyn.* **227**, 280-290.
Pyati, U. J., Cooper, M. S., Davidson, A. J., Nechiporuk, A. and Kimelman, D. (2006). Sustained Bmp signaling is essential for cloaca development in zebrafish. *Development* **133**, 2275-2284.
Qian, F., Germino, F. J., Cai, Y., Zhang, X., Somlo, S. and Germino, G. G. (1997). PKD1 interacts with PKD2 through a probable coiled-coil domain. *Nat. Genet.* **16**, 179-183.
Rasmussen, G. and Rasmussen, C. (1995). Calmodulin-dependent protein kinase II is required for G1/S progression in HeLa cells. *Biochem. Cell Biol.* **73**, 201-207.
Rothschild, S. C., Lister, J. A. and Tombes, R. M. (2007). Differential expression of CaMK-II genes during early zebrafish embryogenesis. *Dev. Dyn.* **236**, 295-305.
Rothschild, S. C., Easley, C. A., Francescatto, L., Lister, J. A., Garrity, D. M. and Tombes, R. M. (2009). Tbx5-mediated expression of Ca^{2+}/calmodulin-dependent protein kinase II is necessary for zebrafish cardiac and pectoral fin morphogenesis. *Dev. Biol.* **330**, 175-184.
Saarikangas, J., Mattila, P. K., Varjosalo, M., Bovellan, M., Hakanen, J., Calzada-Wack, J., Tost, M., Jennen, L., Rathkolb, B., Hans, W. et al. (2011). Missing-in-metastasis MIM/MTSS1 promotes actin assembly at intercellular junctions and is required for integrity of kidney epithelia. *J. Cell Sci.* **124**, 1245-1255.
Sanabria, H., Swulius, M. T., Kolodziej, S. J., Liu, J. and Waxham, M. N. (2009). {beta}CaMKII regulates actin assembly and structure. *J. Biol. Chem.* **284**, 9770-9780.
Sawyer, J. M., Harrell, J. R., Shemer, G., Sullivan-Brown, J., Roh-Johnson, M. and Goldstein, B. (2010). Apical constriction: a cell shape change that can drive morphogenesis. *Dev. Biol.* **341**, 5-19.
Schottenfeld, J., Sullivan-Brown, J. and Burdine, R. D. (2007). Zebrafish curly up encodes a Pkd2 ortholog that restricts left-side-specific expression of southpaw. *Development* **134**, 1605-1615.
Slanchev, K., Putz, M., Schmitt, A., Kramer-Zucker, A. and Walz, G. (2011). Nephrocystin-4 is required for pronephric duct-dependent cloaca formation in zebrafish. *Hum. Mol. Genet.* (in press).
Sullivan-Brown, J., Schottenfeld, J., Okabe, N., Hostetter, C. L., Serluca, F. C., Thiberge, S. Y. and Burdine, R. D. (2008). Zebrafish mutations affecting cilia motility share similar cystic phenotypes and suggest a mechanism of cyst formation that differs from pkd2 morphants. *Dev. Biol.* **314**, 261-275.
Sun, Z., Amsterdam, A., Pazour, G. J., Cole, D. G., Miller, M. S. and Hopkins, N. (2004). A genetic screen in zebrafish identifies cilia genes as a principal cause of cystic kidney. *Development* **131**, 4085-4093.
Tobimatsu, T. and Fujisawa, H. (1989). Tissue-specific expression of four types of rat calmodulin-dependent protein kinase II mRNAs. *J. Biol. Chem.* **264**, 17907-17912.
Tobin, J. L. and Beales, P. L. (2008). Restoration of renal function in zebrafish models of ciliopathies. *Pediatr. Nephrol.* **23**, 2095-2099.
Tombes, R. M., Westin, E., Grant, S. and Krystal, G. (1995). G1 cell cycle arrest and apoptosis are induced in NIH 3T3 cells by KN-93, an inhibitor of CaMK-II (the multifunctional Ca^{2+}/CaM kinase). *Cell Growth Differ.* **6**, 1063-1070.
Tombes, R. M., Faison, M. O. and Turbeville, C. (2003). Organization and evolution of multifunctional Ca^{2+}/CaM-dependent protein kinase (CaMK-II) genes. *Gene* **322**, 17-31.
Torres, V. E., Harris, P. C. and Pirson, Y. (2007). Autosomal dominant polycystic kidney disease. *Lancet* **369**, 1287-1301.
Tsiokas, L. (2009). Function and regulation of TRPP2 at the plasma membrane. *Am. J. Physiol. Renal Physiol.* **297**, F1-F9.
Tsiokas, L., Kim, E., Arnould, T., Sukhatme, V. P. and Walz, G. (1997). Homo- and heterodimeric interactions between the gene products of PKD1 and PKD2. *Proc. Natl. Acad. Sci. USA* **94**, 6965-6970.
Vandorpe, D. H., Chernova, M. N., Jiang, L., Sellin, L. K., Wilhelm, S., Stuart-Tilley, A. K., Walz, G. and Alper, S. L. (2001). The cytoplasmic C-terminal fragment of polycystin-1 regulates a Ca^{2+}-permeable cation channel. *J. Biol. Chem.* **276**, 4093-4101.
Vasilyev, A., Liu, Y., Mudumana, S., Mangos, S., Lam, P. Y., Majumdar, A., Zhao, J., Poon, K. L., Kondrychyn, I., Korzh, V. et al. (2009). Collective cell migration drives morphogenesis of the kidney nephron. *PLoS Biol.* **7**, e9.
Veland, I. R., Awan, A., Pedersen, L. B., Yoder, B. K. and Christensen, S. T. (2009). Primary cilia and signaling pathways in mammalian development, health and disease. *Nephron Physiol.* **111**, p39-p53.
Webb, S. E. and Miller, A. L. (2003). Calcium signalling during embryonic development. *Nat. Rev. Mol. Cell Biol.* **4**, 539-551.
Webb, S. E. and Miller, A. L. (2007). Ca^{2+} signalling and early embryonic patterning during zebrafish development. *Clin. Exp. Pharmacol. Physiol.* **34**, 897-904.
Whitaker, M. (2006). Calcium at fertilization and in early development. *Physiol. Rev.* **86**, 25-88.
Wilson, P. D. (2001). Polycystin: new aspects of structure, function, and regulation. *J. Am. Soc. Nephrol.* **12**, 834-845.
Wilson, P. D. (2004). Polycystic kidney disease. *N. Engl. J. Med.* **350**, 151-164.
Wilson, P. D. (2008). Mouse models of polycystic kidney disease. *Curr. Top. Dev. Biol.* **84**, 311-350.
Wilson, P. D., Geng, L., Li, X. and Burrow, C. R. (1999). The PKD1 gene product, "polycystin-1," is a tyrosine-phosphorylated protein that colocalizes with alpha2beta1-integrin in focal clusters in adherent renal epithelia. *Lab. Invest.* **79**, 1311-1323.
Wingert, R. A. and Davidson, A. J. (2008). The zebrafish pronephros: a model to study nephron segmentation. *Kidney Int.* **73**, 1120-1127.
Wingert, R. A., Selleck, R., Yu, J., Song, H. D., Chen, Z., Song, A., Zhou, Y., Thisse, B., Thisse, C., McMahon, A. P. et al. (2007). The cdx genes and retinoic acid control the positioning and segmentation of the zebrafish pronephros. *PLoS Genet.* **3**, 1922-1938.
Wu, G., Markowitz, G. S., Li, L., D'Agati, V. D., Factor, S. M., Geng, L., Tibara, S., Tuchman, J., Cai, Y., Park, J. H. et al. (2000). Cardiac defects and renal failure in mice with targeted mutations in Pkd2. *Nat. Genet.* **24**, 75-78.
Xia, S., Li, X., Johnson, T., Seidel, C., Wallace, D. P. and Li, R. (2010). Polycystin-dependent fluid flow sensing targets histone deacetylase 5 to prevent the development of renal cysts. *Development* **137**, 1075-1084.
Zhang, T., Kohlhaas, M., Backs, J., Mishra, S., Phillips, W., Dybkova, N., Chang, S., Ling, H., Bers, D. M., Maier, L. S. et al. (2007). CaMKIIdelta isoforms differentially affect calcium handling but similarly regulate HDAC/MEF2 transcriptional responses. *J. Biol. Chem.* **282**, 35078-35087.